Carnegie Mellon University Research Showcase @ CMU

Department of Physics

Mellon College of Science

2008

Electronic states of chemically treated SiC surfaces

Shu Nie

Carnegie Mellon University

Randall M. Feenstra

Carnegie Mellon University, feenstra@andrew.cmu.edu

Y. Ke

University of Pittsburgh

R. P. Devaty

University of Pittsburgh

W. J. Choyke

University of Pittsburgh

Follow this and additional works at: http://repository.cmu.edu/physics

Published In

J. Appl. Phys., 103, 013709.

This Article is brought to you for free and open access by the Mellon College of Science at Research Showcase @ CMU. It has been accepted for inclusion in Department of Physics by an authorized administrator of Research Showcase @ CMU. For more information, please contact research showcase@andrew.cmu.edu.

Electronic States of Chemically Treated SiC Surfaces

Shu Nie and R. M. Feenstra
Dept. of Physics, Carnegie Mellon University, Pittsburgh, PA 15213
Y. Ke, R. P. Devaty and W. J. Choyke
Dept. of Physics and Astronomy, University of Pittsburgh, Pittsburgh, PA 15260

Abstract

Electronic states at chemically treated SiC surfaces have been studied by scanning tunneling spectroscopy. Charge accumulation on the surface is deduced through a voltage shift observed in the spectra. More charge is observed on electro-polished surfaces as compared to untreated (as-received) surfaces. This difference is interpreted in terms of the electro-polished SiC surfaces being more insulating than as-received ones, such that on the former the transport of charge is limited and surface charges cannot come into equilibrium with the bulk semiconductor. Observations of tunneling spectra on SiC prepared by various amounts of hydrogen-etching are used to support this interpretation.

I. INTRODUCTION

Porous SiC has proven to be a useful substrate material for homoepitaxial growth of SiC [1] and heteroepitaxial growth of GaN [2]. Porous SiC has also been found to be a promising material for use as a semi-permeable membrane in biophysics applications [3]. In this latter situation, good biocompatibility of the SiC is revealed by its tendency to maintain clear channels in the membrane, free from clogging or "fouling" [3]. To understand this biocompatibility, knowledge of the surface topographic and electronic properties is important, since these properties play an important role in protein absorption [4,5]. To this end, scanning tunneling microscopy (STM) and spectroscopy (STS) are appropriate tools for investigating the surface properties of porous SiC on the atomic scale.

In this work, we report on the electronic properties of electro-polished p-type 4H-SiC, both C-face and Si-face (these electro-polished surfaces mimic the surfaces of porous SiC, as described below). The observed spectra are found to be very asymmetric, with a usual amount of current at positive voltages but no observable current at negative voltages. We propose that this behavior is due to surface charge accumulating on an incompletely passivated surface (i.e. with enough passivation so that the surface charges are localized from each other, but not enough to produce a zero density of such charges).

To further study this behavior we consider a separate means of surface passivation, namely, H-etching. We prepare a series of samples with varying amounts of H-etching, and we find that the well-etched ones exhibit similar asymmetry in the spectroscopy as the electro-polished samples. In contrast, the samples with minimal H-etching were found to have many more surface states, such that a continuous current flows through the states. Theoretical simulations of the effects of localized surface charges are employed to further investigate this phenomenon. Based on the simulations we estimate for the well-etched samples a negative charge density of about 10¹³ cm⁻² is present on the surface. Similar magnitudes of surface charge density are deduced for the case of the electro-polished surfaces.

Porous SiC is fabricated by the method of electrochemical etching [6]. The electrochemical etching is typically conducted anodically in a hydrofluoric (HF) aqueous solution mixed with ethanol. Depending on current density, surface polarity, doping and electrolyte concentration, electrochemical etching on p-type SiC occurs in one of two regimes: the porous formation regime or the complete dissolution (electro-polishing) regime. Although a main goal of this work is to study the surface spectroscopy of porous SiC, such a study is not possible using scanning probe techniques since the probe tips cannot enter a narrow pore. Therefore, we have performed electrochemical etching in the electro-polishing regime; the chemical reaction is similar to that in the porous formation regime, but material is mainly removed from the substrate surface without creating pores. We have studied electro-polished $(000\ \bar{1})$ and (0001) crystal faces, and we refer to these throughout this paper as C-face and Si-face, respectively.

II. EXPERIMENTAL

Electro-polished samples were prepared from 8° off axis p-type (Al-doped) 4H-SiC, with doping concentrations of 8×10^{18} cm⁻³ for the Si-face and 7×10^{17} cm⁻³ for the C-face. Samples were electro-polished in 1% HF/5% ethanol (weight percentage) for 30 min with current density of 20 mA/cm². The samples were then cleaned in solvent and loaded into an ultra-high-vacuum (UHV) system and baked at 120° C for one day before STM/STS measurement.

For the study of H-etched SiC, samples were cut from an n-type (N-doped) 6H-SiC (0001) wafer with doping concentration of 1×10^{18} cm⁻³. Hydrogen etching was performed by heating the samples in 1 atm of 99.99% pure hydrogen at 10 lpm flow rate, at various temperatures, for 90 seconds ⁷. After H-etching, the samples were exposed to air for about 30 minutes prior to loading into the UHV chamber. Compared with electropolished samples, which were air exposed for more than a month, the brief air-exposure of the H-etched SiC may not produce a homogeneous oxidation of the surface. We therefore intentionally oxidized the H-etched sample following their introduction into the UHV chamber, by exposure to molecular oxygen at 1×10^{-7} Torr for 2 hours with the sample held at 700°C.

As specified above, different doping types were used in our studies of the electropolished and the H-etched samples. This difference was unintentional (the electropolishing requires p-type material, which is relatively rare, whereas the H-etching work was done first and employed commonly available n-type material). This difference in doping type affects the *sign* of the charge accumulation at the surface that we observe in our experiments, but aside from that we do not believe that it significantly affects surface properties. In prior work we have studied UHV-prepared SiC surfaces, both n-type and p-type, and the surfaces were identical in terms of structure and electronic properties [8]. It should also be noted that the polytypes were also different between the electro-polished and the H-etched samples, 4H in the former case and 6H in the latter, again due to availability of the respective materials. But, polytype differences are also expected to have negligible impact on surface properties (other than the height of unit-cell-high steps on the surface [7]), and so this difference should not affect our comparison between the samples.

The morphology of the samples were measured by atomic force microscopy (AFM), performed in air. STM/STS measurements were performed in UHV, at base pressure of

 2×10^{-10} Torr. STM images were acquired at a constant tunneling current of 0.1 nA, using commercially available Pt-Ir tips that were cleaned *in situ* by electron-bombardment using a constant emission current of 1.5 mA and voltage of 300-500 V. For spectroscopic measurements, the differential conductance dI/dV was measured using a lock-in amplifier with modulation voltage of 50 mV. The surfaces of our samples are somewhat inhomogeneous, so that the spectra vary from location to location. To provide an overall view of the spectroscopy we acquire typically a grid of 10×10 spectra over an area of 20×20 nm² and we plot all the spectra together in a single graph, thus permitting a convenient view of the main features of the spectra [9].

Our spectra are generally measured using a variable tip-sample separation in order to enhance the values of the conductance, thereby achieving a large dynamic range in the experiment [10]. In particular, as the voltage V is swept from some starting voltage V_1 to an ending voltage with opposite sign V_2 , the separation is changed according to $\Delta s = -a_1 |V - V_1|$ as V changes from V_1 to 0 and then $\Delta s = -a_1 |V_1| + a_2 |V - V_2|$ as V changes from 0 to V_2 , where a_1 and a_2 are positive constants. The values of a_1 and a_2 are chosen during the measurement in an effort to magnify the conductance to a conveniently measurable value, with both of them usually having values of about 0.1 nm/V.

In a typical tunneling situation, data acquired as described above can be normalized to constant separation simply by multiplying it by $\exp(2\kappa \Delta s)$, using a value of κ appropriate to an ideal tunneling barrier of about 11 nm⁻¹. However, for the data presented in this work, in which nonequilibrium effects (surface charging) are sometimes large, the values of κ deviate substantially from this ideal value. Not only are the measured κ values different between positive and negative voltages, but they also can have significant voltage dependence even for a given sign of the voltage. For this reason, we present all of our conductance data in their as-measured form, and we display the Δs curve used for the measurement along with the respective spectra. From the subsequent results of Section III(C) concerning κ values, it is possible (for comparison purposes) to normalize the data to constant separation if desired.

III. RESULTS

A. Electro-polished surfaces

In this section we describe our results for the electro-polished p-type SiC, both C-face and Si-face. The electro-polishing was performed in the same manner for the two types of samples, as discussed in Section II, although the morphological results are somewhat different as shown in Fig. 1. The electro-polished C-face, Fig. 1(a), has many small depressions on the surface while fewer such features are seen on the Si-face, Fig. 1(b). To interpret this difference, we refer to the work of Shishkin et al. who systematically studied photoelectrochemical etching of C-face and Si-face SiC [6]. When the Si-face of a p-type SiC sample is exposed to the anodizing conditions, electro-polishing of the crystal occurs for HF concentrations in the range from 1% to 20%. In contrast, for the C-face, electro-polishing occurs only at HF concentrations of 1% or below, with porous structures forming at higher concentrations. Since our etching of both surfaces were performed at 1% HF, we expect the C-face etching to be much closer to the condition for

pore formation than the Si-face. This expectation is in agreement with the observed morphologies of the images, with the C-face showing many more nascent pores.

Tunneling spectra from the electro-polished surfaces are shown in the lower panels of Fig. 2, with the upper panels indicating the relative sample-tip separations used for each measurement. Note that the dI/dV values are shown with a logarithmic scale, and that the horizontal axis is the sample voltage relative to the probe tip. The latter, in the absence of semiconductor band bending effects that vary with the sample voltage, represents the energy of a state relative to the Fermi-level. For the C-face, the tunneling current at negative voltages is too low to be detected for voltages as low as -10 V, Fig 2(a). Similar spectra are observed for the Si-face, Fig. 2(b), although the range of the measurement is somewhat more restricted in that case.

Our explanation for the lack of observable current at negative voltages is based on band bending in the semiconductor, as will be discussed in Section IV. We propose that the electro-polished surface possess traps at the surface into which charge from the tunnel current accumulates. The number of these traps is sufficiently small so that the trapped charge cannot flow away from the tunnel junction along the surface (i.e. on the time scale of the measurement) and hence it produces the band bending in the semiconductor. We test this hypothesis in the following section by utilizing hydrogen-etched SiC.

B. Hydrogen-etched surfaces

We propose that the absence of detectable tunneling current at negative sample voltage on electro-polished SiC is due to band bending induced by charge accumulation at the surface. Since it is difficult to control the electro-polishing, i.e. to only partially polish a surface, we use another system to illustrate the development of the band bending as the number of surface defects (traps) is varied. In particular, we use SiC that has been Hetched at various temperatures.

An AFM image of an as-received n-type SiC(0001) wafer (6H, Si-face) is shown in Fig 3(a). Many residual polishing scratches are apparent on the surface, in agreement with prior studies of such wafers [7,11]. STS data, shown in Fig. 4(a), was collected on the as-received sample without further treatment except for degassing. An apparent band gap of about 1.5 eV is seen in the spectra, considerably smaller than the bulk band gap 3.0 eV. Many mid-gap states are thus present on this as-received sample, arising from surface defects associated with the polishing damage (along with oxidation from air exposure). The Fermi level (0 V) is seen to be pinned near mid-gap.

When we partially H-etch the 6H-SiC(0001), at a temperature of about 1400°C, the polishing damage is partly but not completely removed, as shown in Fig 3(b). Spectral results are shown in Fig. 4(b) for this surface after intentional oxidation. The band gap is seen to open up compared to Fig. 4(a), with an apparent gap of about 2.5 eV at the minimum measurable conductance values. It is also notable that the conduction band (positive voltage) conductance values are very much smaller than those in the valence band (negative voltages), and the conduction band edge has clearly been shifted up to higher voltages.

When we fully etch the SiC, at about 1700°C, the AFM images reveal atomically flat terraces separated by steps [7,11], as shown in Fig 3(c). STS results for this surface after intentional oxidation are displayed in Fig. 4(c). A further increase in the size of the band

gap is seen, with the apparent conduction band edge shifting up to even higher voltages, around 5 V.

Summarizing the above results, we find that H-etching reduces the density of defects on the surface, as apparent in both the morphology and the number of mid-gap states found in spectroscopy. For a well-etched surface we find negligible tunneling current in the band gap region. Additionally, the onset of the conduction band shifts upwards in voltage as the amount of etching (i.e. degree of surface perfection) increases. Importantly, these data on the H-etched SiC were acquired on n-type wafers, whereas the study of the previous Section on electro-polished samples was performed on p-type wafers. Hence, the shifts in the conduction band edge observed here are analogous to the shifts in the valence band edge found in the previous section. In both cases, as will be discussed in Section IV, we explain the shift in the band edges as a consequence of transport limitations in the flow of the surface charges, producing fixed charge on the surface that acts to shift the apparent band edge in the spectra.

C. Inverse decay length measurements

In addition to the spectral results of the prior Sections, another means of probing the characteristics of the tunnel junction (and hence the semiconductor surface) is to measure the inverse decay length, κ , of the tunneling process. The dependence of the tunneling current on sample-tip separation is, to a good approximation, given by $I = I_0 \exp(-2\kappa x)$, where s is the sample-tip separation. For an ideal vacuum tunneling barrier κ has a value given by $\sqrt{2m\phi}/\hbar = 11 \text{ nm}^{-1}$ where m is the free electron mass and where we have used an average work function ϕ between tip and sample of 4 eV. In practice, observed values of κ may be less than this value due to various types of nonideal behavior of the tunnel junction.

We have measured κ at various voltages for our samples. For large positive voltages on the p-type electro-polished samples or large negative voltages on the n-type H-etched samples, we find κ values close to the ideal one. An example is shown in Fig. 5, acquired with a sample-tip voltage of +3 V, on a C-face electro-polished sample.

Considering now the results over a wider range of voltages, Fig. 6 shows the results for κ obtained from the as-received and H-etched samples. For large negative sample voltages, near -3 V, the κ value is relatively close to the ideal one. As the voltages get smaller in magnitude the κ values decrease significantly, as will be further discussed in Section IV. However, for positive voltages, the κ value is quite small throughout the entire voltage range. We find similar behavior on the electro-polished samples (but with the sign of the voltages reversed). In general, whenever the conductance values show a marked decrease and the band onsets shift out to voltages with higher magnitude, then the accompanying κ values become quite small.

IV. DISCUSSION

In this section we discuss our interpretation for the observed spectral results. The most striking feature in the observed spectra is that for p-type material the tunnel current into the valence band is very small (unobservable) and for n-type material the current into the conduction band is very small. In the latter case we have observed the progression of this effect as the number of surface states is varied.

Our model for the observed spectra is illustrated in Fig. 7, considering for ease of discussion the n-type situation. Proposed band bending diagrams for positive and negative sample-tip voltages are shown in Figs. 7(a) through (d). For the case of positive voltages, a large amount of band bending is apparent in the spectra. We attribute this to band bending in the semiconductor due to the accumulation of negative charge (electrons, from the tunnel current) at the surface, as pictured in Figs. 7(a) and (b). In this situation, the surface of the semiconductor is *not* in equilibrium with the bulk, i.e. their Fermi levels are different. The trapped charges on the surface can in principle flow away from the tunnel junction, both along the surface and into the semiconductor, with the latter occurring by tunneling through the band gap as shown by J_S in Fig. 7. But on the basis of the observed data for positive sample voltages we conclude that these processes are too slow to establish equilibrium between the surface and the bulk.

As the positive sample voltage increases, the average height of the vacuum barrier decreases and additional charges are accumulated on the surface, as pictured in Fig. 7(b). The current into the bulk semiconductor, J_S, increases and/or the current flowing on the surface away from the tunnel junction increases. At some point these currents become sufficiently large that the amount of surface charge and the band bending increases less rapidly with voltage, and hence the vacuum tunnel current increases and becomes observable. (It should be noted that for the large band gap of SiC, current flow between conduction and valence bands, i.e. semiconductor inversion, is negligible for the voltages considered here [12]).

For small negative sample-tip voltages, shown in Fig. 7(c), a small amount of upwards band bending will still occur due to the presence of surface states (which accept negative charge from the donors in the bulk). This upwards band bending again results in relatively small values of $J_{\rm S}$ and thus, as for positive voltages, the surface Fermi-level can be different than in the bulk and the amount of band bending changes significantly with the applied sample voltage. Hence, as shown in Fig. 6, the inverse decay length measured at small negative sample voltages is less than the ideal value.

For large negative sample-tip voltages on n-type material, Fig. 7(d), the situation is somewhat different. In this case the band bending decreases enough to become zero or slightly negative. Charge accumulation on the surface would involve positive charge in this case. But, once the band bending approaches these flat-band conditions it will not decrease further, since the current J_S flowing from the conduction band is large enough to provide a source of negative charge for the surface and hence balance any further removal of surface charge by the tunnel current.

Some additional comment is merited for the case of the positive voltages, Figs. 7(a) and (b), concerning the relationship between the vacuum tunnel current and the surface charge. Consider starting from some given sample voltage where the current is observable, and then increasing the voltage by, say 1 V. In the absence of further band bending this voltage increase would lead to a large (order-of-magnitude) increase in the tunnel current. However, such a large increase in current would also lead to a higher occupation of the surface states, thus increasing the band bending and *decreasing* the tunnel current (since fewer states are available to tunnel into). Thus, the resulting increase in current due to the 1V voltage increment is much smaller than would be seen in the absence of the changing band bending. Hence, in the data only a very gradual increase in current with voltage is observed.

The above type of argument can also be applied to the situation of a change in the tip-sample separation, i.e. as performed during a measurement of κ . Again, a decrease in the separation should lead to a large increase in current, but that in turn will produce additional occupation of the surface states which will produce an increase in the band bending and hence a decrease in the current. In this way, the small values observed for κ at positive voltages and small negative voltages for n-type material can be understood.

On electro-polished 4H-SiC, we also see spectra similar to those for the oxidized H-etched SiC, allowing for the difference between the n-type and p-type wafers in the two cases. We therefore attribute the behavior of the spectra to the same origin: accumulation of surface charges due to the presence of surface defects.

Of course, if there is a zero density of states on the surface, then the band bending and associated voltage shifts described above will not occur. Some band bending will still occur in the semiconductor due simply to the *electrostatic* charge distribution on the tip (i.e. arising from the voltage difference between tip and sample [13]), but this is a relatively small effect compared to the large shifts found in the present data. The fact that we observe a larger shift for a more passivated surface [Fig. 4(c) compared to Figs. 4(b) or (a)] indicates that we are in the regime where the density of surface states is high enough to produce significant charging, but that transport between neighboring states is still a significant factor in establishing equilibrium across the surface.

To estimate the amount of surface charge that produces the observed shifts in the band edges, we perform a tunneling computation for a metallic probe-tip in proximity to a doped semiconductor [14]. We assume a tip radius of 30 nm and tip-sample separation of 0.8 nm which are typical in STS experiments, and for the semiconductor we take a band gap of 3 eV and doping density of 1×10^{18} cm⁻³. The contact-potential (work-function difference) between tip and sample to taken to be 0 eV. We first consider a surface without any surface states and hence no surface charge, with the resulting conductance vs. voltage relationship shown by the solid line in Fig. 8 [15]. Now, if we assume a constant amount of fixed negative charge on the surface, the conduction band onset shifts as shown by the dashed lines in the figure. Large shifts on the order of 5 V occur for fixed charge density of about 1×10^{13} cm⁻².

Comparing the results of Fig. 8 with the experimental results, we find e.g. for the fully H-etched results that the observed shift in the conduction band onset is due to a surface charge density with magnitude of about 1×10^{13} cm⁻². Considering now the electropolished samples, where we do not observe any valence band current, the fixed surface charge density (positive in this case) would have a density at least this large. We do not however expect a density much larger than this, since in that case hopping conduction between the surface states would start to become observable. For the as-received samples we expect a rather high surface state density, perhaps 10% or more of the density of dangling bonds on bulk terminated surface (i.e. 10% or more of 1.22×10¹⁵ cm⁻²), and in this case we find that the surface defects form a conducting band. Thus, in summary, we find that both the H-etched and the electro-polished surfaces are *passivated*, with most of the dangling bonds that appear on an as-received surface (or that would be present on a bulk-terminated surface) being saturated, but with some small fraction of these dangling bonds remaining and giving rise to mid-gap electronic states.

Transport limitations in current flow away from a tunnel junction have been reported in several prior works. For example, asymmetric spectra were observed on air-exposed ntype and p-type Si(100) by LaBrasca et al. [16]. Although the voltage range of those spectra is quite limited compared to the present study, the asymmetry of the spectra is the same as observed here. In a separate work, tunneling spectra of UHV-prepared SiC(0001)- $\sqrt{3} \times \sqrt{3}$ R30° surfaces by Ramachandran and Feenstra revealed a strong dependence on the magnitude of the current, interpreted in terms of a "spreading resistance" in the transport of carriers to (or from) surface states [8]. Again, the results are analogous to those reported in the present work, except that the surface states in that case were *intrinsic* to the surface reconstruction rather than resulting from defects on the surface. Limitations in current transport due to charging of *extrinsic* (defect-derived) states has been reported previously on the Ge(111)-c(2×8) surface [12], although the effects in that case were relatively small compared to the present ones on SiC since the density of defects was very much smaller.

Examining prior work dealing with porous SiC, using deep level transient spectroscopy (DLTS) Look et al. have reported a new type of deep trap associated with the internal surfaces of the pores [17]. The trap has acceptor character, becoming negatively charged when occupied, with energy level at about 0.8 eV below the conduction band minimum. The density of such traps on the porous surfaces was found to be about 2.5×10^{12} cm⁻². The DLTS measurements allow a spectroscopic location of the energy levels, something which is not achieved in our tunneling spectroscopy for the well passivated surfaces (electro-polished, or fully H-etched) since insufficient current flows through the traps to permit direct observation of their energy levels. In this respect, the STS results of the present work bear more resemblance to the well known voltage shifts seen in capacitance-voltage characteristics of metal-oxide-semiconductor structures [18], in which fixed charge in the oxide produces a voltage shift in the characteristic.

Finally, concerning the biocompatibility of porous SiC (an explanation of which was one motivation for the present work), our results have demonstrated that the electropolished surface is quite insulating (even though it contains a significant number of fixed charges). In this regard, adsorption of proteins on a surface is known to involve electron transfer to/from the surface [5], and hence an insulating surface would inhibit this process. This nature of the electro-polished SiC surface may provide an explanation for the known biocompatibility of the surface [19].

V. CONCLUSION

Morphology and electronic properties of electro-polished p-type SiC(0001) surfaces have been investigated by AFM and STM/STS. Negligible tunneling current is found at negative sample voltages, which is interpreted in terms of band bending in the semiconductor due to charge accumulation at the surface. STS of SiC prepared by various amounts of hydrogen-etching is used to support this interpretation. Comparison with tunneling computations reveals a density of about 10¹³ cm⁻² fixed charges on both the electro-polished and the H-etched surfaces. Compared to an untreated (as-received) surface that displays large conduction through mid-gap states, the electro-polished or H-etched surfaces are found to be relatively insulating with the vast majority of dangling bonds saturated on the surface. Nevertheless, a few percent of dangling bonds remain and form mid-gap states, which become occupied due to the tunnel current and lead to the observed band bending in the spectra.

ACKNOWLEDGMENTS

This work was supported by a Defense University Research Initiative on Nanotechnology (DURINT) program administered by the Office of Naval Research under grant N00014-01-1-0715 (program monitor Colin Wood).

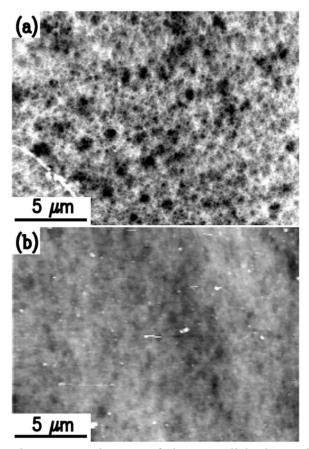


Fig. 1 AFM images of electro-polished 4H-SiC: (a) the $(000\,\overline{1})$ surface (C-face), and (b) the (0001) surface (Si-face), both displayed with a grayscale range of 33 nm.

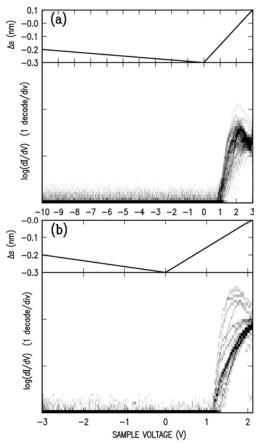


Fig. 2 Tunneling spectra of electro-polished p-type 4H-SiC: (a) C-face, and (b) Si-face. Lower panels are multi-spectra plots and the upper panels are the corresponding sample-tip separation used during the measurement. Note the different scales on the horizontal axes.

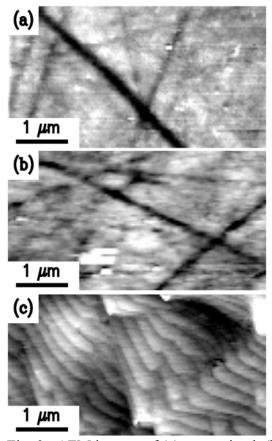


Fig. 3 AFM images of (a) as-received, (b) mildly H-etched, and (c) fully H-etched 6H-SiC, displayed with grayscale ranges of 10, 8, and 3 nm, respectively.

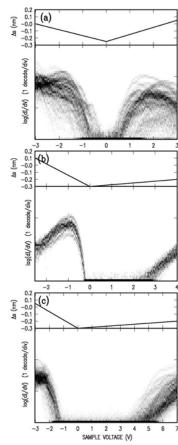


Fig. 4 Spectra of oxidized H-etched 6H-SiC(0001): (a) as-received, (b) mildly H-etched, and (c) fully H-etched. Note the different scales on the horizontal axes.

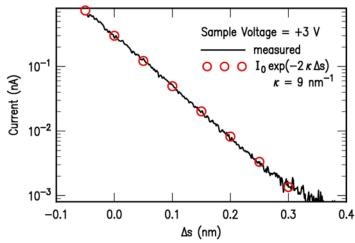


Fig. 5 (color online) Tunnel current vs. change in tip-sample separation, for a sample voltage of +3V, on the electro-polished C-face. The solid line shows measured data and the open circles show an exponential fit.

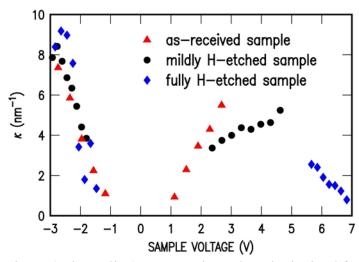


Fig. 6 (color online) Inverse decay length obtained from n-type 6H-SiC samples, as-received and with various amounts of H-etching.

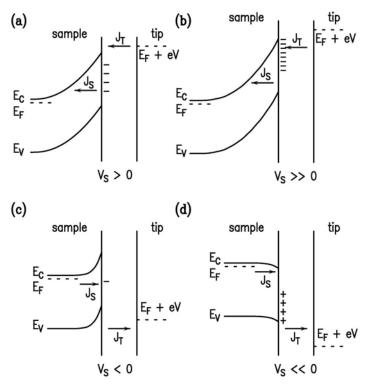


Fig. 7 Schematic diagram of charge accumulation due to transport limited current on an n-type SiC surface at (a) small positive sample voltage, (b) large positive sample voltage, (c) small negative voltage, and (d) large negative voltage. E_C is the conduction band minimum, E_V is the valence band maximum, and E_F is the Fermi level of the bulk semiconductor. J_T is the tunneling current through the vacuum and J_S is the current flowing to/from the bulk of the semiconductor (the directions of the arrows indicate electron flow).

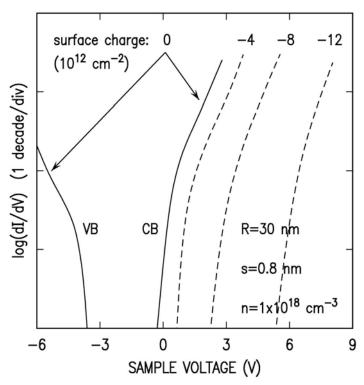


Fig. 8 Computed tunneling characteristics for a metal probe tip in proximity to a semiconductor. The solid lines give the result with zero surface charge, showing the valence band (VB) and conduction band (CB) onsets. The dashed lines show the CB onset assuming various amounts of fixed negative surface charge, as indicated.

REFERENCES

_

¹ J. E. Spanier, G. T. Dunne, L. B. Rowland, and I. P. Herman, Appl. Phys. Lett., **76**, 3879 (2000).

² C. K. Inoki, T. S. Kuan, C. D. Lee, Ashutosh Sagar, and R. M. Feenstra, Mat. Res. Soc. Symp. Proc. Vol. **722**, K1.3.1 (2002).

³ A. J. Rosenbloom, Y. Shishkin, D. M. Sipe, Y. Ke, R. P. Devaty, and W. J. Choyke, Mat. Sci. Forum **457-460**, 1463 (2004).

⁴ R. Emch, M. Jobin, F. Zenhausern, S. Steinemann, and P. Descouts, J. Vac. Sci. Technol. B **9**, 1263 (1991).

⁵ A. Rzany and M. Schaldach, Prog. Biomed. Res. **1**, 59 (1999).

⁶ Y. Shishkin, Y. Ke, R. P. Devaty, and W. J. Choyke, J. Appl. Phys. **97**,44908 (2005).

⁷ V. Ramachandran, M. F. Brady, A. R. Smith, R. M. Feenstra, and D. W. Greve, J. Electron. Mater. **27**, 308 (1998).

⁸ V. Ramachandran and R. M. Feenstra, Phys. Rev. Lett. **82**,1000 (1999).

⁹ Multiple spectra are plotted on a single graph using the following method: The twodimensional expanse of the graph is divided into pixels, and a two-dimensional histogram is used to record values for each pixel. When a plotted spectrum crosses a given pixel, the histogram value for that pixel is incremented. After all spectra are plotted, grayscale values are assigned according to the histogram values and the result is presented as a gray scale image.

¹⁰ R. M. Feenstra, Phys. Rev. B **50**, 4561 (1994).

S. Doğan, D. Johnstone, F. Yun, S. Sabuktagin, J. Leach, A. A. Baski, H. Morkoç, G. Li, and B. Ganguly, Appl. Phys. Lett. 85, 1547 (2004).

¹² R. M. Feenstra, S. Gaan, G. Meyer and K. H. Rieder, Phys. Rev. B **71**, 125316 (2005).

¹³ R. M. Feenstra, J. Vac. Sci. Technol. B **21**, 2080 (2003).

¹⁴ R. M. Feenstra, Y. Dong, M. P. Semtsiv, and W. T. Masselink, Nanotechnol. **18**, 044015 (2007).

For simplicity and clarity of presentation we have neglected the "dopant-induced" component in the tunneling current arising from electron occupation of the conduction band due to the doping [see R. M. Feenstra and J. A. Stroscio, J. Vac. Sci. Technol. B 5, 923 (1987)]. This component certainly does *not* occur in the experiment because there are sufficient numbers of surface states so that such occupation does not occur until very large negative voltages, and in the theoretical curve for zero surface charge density we neglect it since it obscures the onset of the valence band edge.

J. LaBrasca, R. Chapman, G. McGuire, and R. Nemanich, J. Vac. Sci. Technol. B 9, 752 (1991).

¹⁷ D. C. Look, Z-Q. Fang, S. Soloviev, T. S. Sudarshan, and J. J. Boeckl, Phys. Rev. B 69, 195205 (2004).

¹⁸ S. M. Sze *Physics of Semiconductor Devices*, 2nd ed. (Wiley, New York, 1981), p. 391

¹⁹ C. Harder, A. Rzany, M. Schaldach, Prog. Biomed. Res. **1**, 71 (1999).